Journal of Photochemistry & Photobiology, A: Chemistry 414 (2021) 113286

Contents lists available at ScienceDirect

Journal of Photochemistry & Photobiology, A: Chemistry

journal homepage: www.elsevier.com/locate/jphotochem

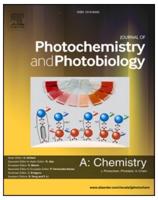

Cyclobutane-cleavage of *anti*-head-to-head coumarin and quinolinone homo- and cross-dimers via single- and two-photon-absorption photochemistry

Nikolai Bieniek, Sebastian Inacker, Hee-Cheol Kim, Norbert Hampp *

Department of Chemistry, University of Marburg, Hans-Meerwein-Straße 4, D-35032, Marburg, Germany

ARTICLE INFO

Keywords:
Coumarin
Quinolinone
Homo-dimer
Cross-dimer
Cycloreversion
Twophoton-absorption

ABSTRACT

The light-driven cleavage of cyclobutane containing systems via [2 + 2] cycloreversion, such as di-coumarin, is an important yet poorly investigated photochemical reaction. Its applications can be found in smart crosslinking polymers or light-activated drug release. We report the increased cleavage efficiencies of the coumarins lactam analog quinolinone for single-photon as well as two-photon-absorption experiments. To investigate the structure-function relationship of the molecular substitution pattern and its influence on the photoactivity, a coumarin-quinolinone cross-dimer was synthesized and investigated towards its cleavage efficiencies in single-photon as well as two-photon photocleavage. The cross-dimer shows a lower cleavage efficiency than both homo-dimers. The presented results are of interest, e.g., for applications utilizing highly efficient cleavage reactions in symmetric or asymmetric molecular frameworks.

1. Introduction

The photochemical and photophysical properties of coumarin and its derivatives have been intensively studied within the last decade since the first report of a light-driven [2 + 2]cycloaddition by Ciamician and Silber [1]. Irradiation of coumarin with low energy UV-light ($\lambda > 300$ nm) leads to the formation of cyclobutane-type dimers with altered chemical and physical properties compared to the monomers. Up to four different isomers of the dimeric species can be obtained [2]. The distribution between those is influenced by several factors, as solvent polarity, triplet sensitization, or concentration of the monomeric species [3]. The obtained dimers revert to their monomeric form upon irradiation with light of appropriate wavelength ($\lambda < 300$ nm) [4]. The broad field of applications utilizing this reversible photochemical behavior includes crosslinking in photoactive polymers [5], photo-alignment of liquid crystals [6], controlled release of small molecules from host complexes [7], and drug-release from polymer-bound structures [8]. Further developments within this field require a deeper understanding of parameters influencing the underlying chemical and physical mechanisms. Previous research on coumarin dimers investigated the stereochemical influences [9], influences of the substitution pattern [10,11], and the effects of single- and two-photon absorption on the cyclobutane cleavage efficiencies [12].

The coumarins lactam analog, 1-methylquinolin-2(1*H*)-one (NMQ), and its derivatives find several applications in biomedical chemistry [13–15]. Despite these, the list of publications dealing with its photochemical properties is short, mainly focusing on the dimerization kinetics [16,17]. Quinolinones show a more efficient intersystem crossing (ISC) than the coumarins, leading to higher rate constants and quantum yields for the [2 + 2]-cycloaddition. Previous work on the cyclobutane cleavage of the quinolinones *syn*-head-to-tail dimer demonstrates the influence of lactone- to lactam-substitution. The corresponding NMQ dimers undergo different mechanistic pathways leading to the parent monomeric forms compared to the coumarin dimers [18].

This work reports on the cyclobutane cleavage reactions of coumarin and quinolinone *anti*-head-to-head dimers (Fig. 1) and compares the single-photon (SPA) and two-photon-absorption (TPA) characteristics of both. As the homo-dimers show great differences regarding their cyclobutane cleavage efficiency, we decided to study the cleavage experiments of a hybrid cross-dimer, containing both structural motifs. We found significant deviations from the expected kinetics during single-photon experiments as well as during two-photon experiments. In both cases the photochemical and photophysical performance of the cross-dimer is mainly influenced by the coumarin-motif of the molecular

---

* Corresponding author.
E-mail address: hampp@uni-marburg.de (N. Hampp).

https://doi.org/10.1016/j.jphotochem.2021.113286
Received 26 January 2021; Received in revised form 30 March 2021; Accepted 31 March 2021

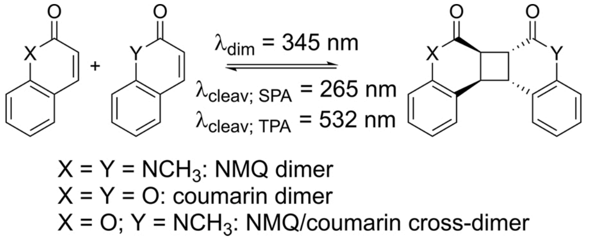

Fig. 1. Irradiation of NMQ and/or coumarin with 345 nm leads to the formation of either the corresponding homo-dimers or the hybrid cross-dimer. Cyclobutane cleavage was carried out via single photon absorption (SPA) and two photon absorption (TPA).

framework, canceling out the improved properties brought into the system by the lactam group.

2. Experimentals

2.1. Materials

Coumarin (Acros Organics, 99 %), DMAP (Sigma Aldrich, 99 %), *N*-Methylaniline (VWR, 99 %), triethylamine (VWR, 99 %), aluminum chloride (Roth, 98 %), sodium chloride (Fischer Chemical, 99.5 %), magnesium sulfate (Grüssing, 99 %), *p*-toluenesulfonic acid monohydrate (Alfa Aeasar, 98 %), dichloromethane (Acros Organics, 99.8 %), acetonitrile gradient grade (Riedel de Haen, 99.9 %) and concentrated hydrochloric acid (VWR) were used as received. All other solvents were of technical quality and purified by distillation before use.

2.2. NMR-spectroscopy

^{1}H NMR spectra of the monomers were recorded on an AV-300 (Bruker, 300 MHz) and an AV-500 (Bruker, 500 MHz) for the dimers. Dimethyl-sulfoxide-d_6 and acetonitrile-d_3 were used as solvents. The δ chemical shift scale was calibrated using the residual solvent peaks.

2.3. UV/Vis-spectroscopy

UV/Vis-spectra were recorded on a photo spectrometer Lambda35 (PerkinElmer). The analytes were dissolved in acetonitrile and the solutions were measured in quartz cuvettes with a pathlength of 1 cm and a volume of 2 mL.

2.4. Chromatography

HPLC analysis was performed on an Ultimate 3000 system (Dionex) equipped with a diode array detector. An RP-18 column was used with a 60:40 (v/v) mixture of acetonitrile and water (acidified with 300 μL H_3PO_4 /L) as eluent at a flow rate of 1 mL/min. For thin-layer chromatography, Merck Silica Gel 60 F_{254} plates were used. Flash column chromatography was carried out on Macherey Nagel silica gel 60, 0.063 – 0.2 mm.

2.5. Mass spectrometry

HR-ESI mass spectra were acquired on an LTQ-FT Ultra mass spectrometer (Thermo Fischer Scientific) using acetonitrile as solvent.

2.6. Synthesis of N-Methyl-N-phenylcinnamide

The NMQ precursor was synthesized via a modified literature procedure [19]. 20.00 g (120.00 mmol, 1.00 eq) cinnamoyl chloride was dissolved in dry 50.00 mL dichloromethane. 16.63 mL triethylamine (12.14 g, 120.00 mmol, 1.00 eq) and catalytic amounts of DMAP were added. The solution was cooled to 0 °C and 12.97 mL *N*-Methylanilin (12.85 g, 120.00 mol, 1.00 eq) were added dropwise. The ice bath was removed and the solution was stirred for 2 h. After completion, as checked via TLC (DCM:MeOH 30:1), water was added and the phases were separated. After washing with sat. NH_4Cl solution, water, and brine the organic phase was dried using $MgSO_4$ and filtered off. The solvent was removed, resulting in 21.64 g (91.20 mmol, 76 %) of a yellow solid, which was used for the next step without further purification. Analytics are in accordance with the literature [19].

2.7. Synthesis of N-methylquinolinone

NMQ was synthesized via a modified literature procedure [19]. A solid mixture of 1.00 g (4.21 mmol, 1.00 eq) *N*-Methyl-*N*-phenylcinnamide and 1.69 g (12.64 mmol, 3.00 eq) anhydrous aluminum chloride were heated to 110 °C until a dark-colored melt formed. The melt was heated for 10 min, before cooling to room temperature. After the addition of an excess of ice-cold water, a solid formed. The solid was filtered off and dissolved in ethyl acetate. The organic phase was washed with 5% aq. HCl, water, brine, and dried over $MgSO_4$ and filtered. Removing the solvent under reduced pressure and drying in a fine vacuum resulted in 0.58 g (3.64 mmol, 87 %) of a yellow solid. Analytics are in accordance with the literature [19].

2.8. Preparative dimerization reactions in flow

Dimerization reactions were performed in a homemade photochemical reactor consisting of two LED-Arrays (35.4 W each, Neumüller electronics, custom-designed) at 345 nm and a spiral FEP-tube with an inner diameter of 0.5 mm and an outer diameter of 1/16 inch in between two 2 mm thick glass slides. The length of the tube spiral is 18.57 m, resulting in a total irradiated volume of 3.56 mL. The total number of photons was $6.86 \pm 0.1 \cdot 10^{17}$ photons·s^{-1} as determined by actinometry of azobenzene [20,21]. The solution was pumped through the reactor using a HPLC-pump (Shimadzu LC-10AS) and a back pressure regulator (Vici Jour JR-BPR2).

2.9. Synthesis of anti-head-to-head coumarin dimer

The coumarin dimer was prepared as previously described [9]. Yield: 35 %.

2.10. Synthesis of anti-head-to-head NMQ dimer

A solution of NMQ (10 mM) in acetonitrile was pumped through the flow reactor at a flow rate of 0.75 mL/min, resulting in a reaction time of approx. 5 min. After solvent evaporation, the crude product was recrystallized from ethanol and dried in vacuo to yield the *anti*-head-to-head NMQ dimer. Analytics are in accordance with the literature [22]. The *anti-head-to-head* structure was determined via single crystal X-Ray diffraction [23]. Yield: 81 %.

2.11. Synthesis of anti-head-to-head NMQ/Coumarin cross-dimer

In a typical procedure, a 50 mM solution of NMQ and coumarin in acetonitrile was pumped through the flow reactor at a flow rate of 0.20 mL/min, resulting in a total reaction time of approx. 18 min. After completion, the solvent was removed under reduced pressure and a solid was received consisting of NMQ/coumarin cross-dimer as the major product, and the NMQ dimer as the minor product. The coumarin dimer could only be found in traces as analyzed by HPLC. For the removal of the monomeric compounds and the coumarin dimer, the solid was recrystallized from Ethanol. The remaining solid (NMQ dimer and NMQ/coumarin cross-dimer) was then refluxed in MeOH (+ cat. HCl) overnight to open the lactone-ring of the cross-dimer. After evaporation to dryness, the ring-opened derivative and the NMQ dimer could be easily separated by column chromatography using pentane/ethyl acetate 3:2 as eluent. For re-lactonization it was refluxed overnight in toluene with 5 mol% TsOH$\cdot$$H_2O$. After completion, as checked by TLC, the mixture was absorbed on silica and purified via column chromatography using pentane/ethyl acetate 2:1 as eluent. The overall yield of the resulting colorless solid was 25 % compared to the monomeric species. Analytics are in accordance with the literature [24]. The *anti-head-to-head* structure was determined via single crystal X-Ray diffraction [25].

2.12. Single-photon-absorption (SPA) induced photocleavage

5 mM solutions of the dimers were irradiated at 265 nm using a 10 mW UV-LED (Thorlabs). The incident light intensity at the corresponding wavelength was $I_{SPA} = 1.87 \cdot 10^{15}$ photons$\cdot$s^{-1}. The photon count per second was determined utilizing the azobenzene actinometric system as a reference [20,26]. The irradiated area was 1.8 cm^2.

2.13. Two-photon-absorption (TPA) induced photocleavage

5 mM solutions of the corresponding dimers were irradiated with 532 nm pulses of 3 ns duration from an Infinity 40–100 (Coherent) mode-locked Nd:YAG laser system. An infrared filter was placed between the irradiation system and the sample. The beam diameter was 4.8 mm, the repetition rate was 20 Hz. Light intensity was determined with a laser power meter (FieldMax II equipped with a PM-100−19C-sensor, Coherent Inc.).

2.14. Tracing of photoconversion

Photocleavage was monitored via UV/Vis absorption spectroscopy using a Lambda35 (PerkinElmer) spectrometer. A sample containing the parent unirradiated solution was used as a reference to determine the absorption change

3. Results and discussion

3.1. UV/Vis absorption spectroscopy

The obvious difference between dimeric and monomeric moieties is an unsaturated double bond along the α-, β-carbonyl position in the latter. This structural difference affects the spectral properties of the considered molecules. The absorption spectra of NMQ, coumarin, and the corresponding homo- and cross-dimers are given in Fig. 2.

The main difference is the missing absorption above 300 nm due to the lack of the double bond across the α-, β-carbonyl position in the dimeric species. Among the three considered dimers, the coumarin shows the weakest absorption between 250 nm and 300 nm. The two dimers containing at least one lactam group show a higher absorption in this wavelength range, with absorption even beyond wavelengths above 300 nm. This bathochromic shift can be assigned to the electron-donating effect of the amide function.

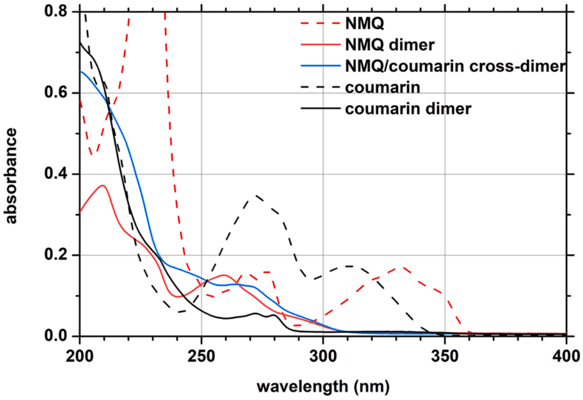

Fig. 2. UV/Vis spectra of monomeric (0.030 mM) and dimeric (0.015 mM) NMQ and coumarin species measured against acetonitrile as reference.

3.2. SPA induced cyclobutane cleavage

SPA cleavage of coumarin dimers is described in the literature [27]. This work focuses on photocleavage of the *anti*-head-to-head NMQ dimer and the *anti*-head-to-head NMQ/coumarin cross-dimer, which is first described here. Photocleavage of these dimers was analyzed by following the increase of absorbance at 332 nm and 318 nm, respectively, via UV/Vis-spectroscopy. The results are presented in Fig. 3.

Both dimers undergo cycloreversion upon being irradiated with 265 nm light. Considering the applied energy, it is remarkable that both homo-dimers cleave into their parent monomeric forms more efficiently than the hybrid cross-dimer. The increasing monomer concentration for the three considered dimers depending on the applied photon energy is plotted in Fig. 4.

To determine the photoconversion for the cross-dimer, the Beer-Lambert law for substance mixtures must be applied:

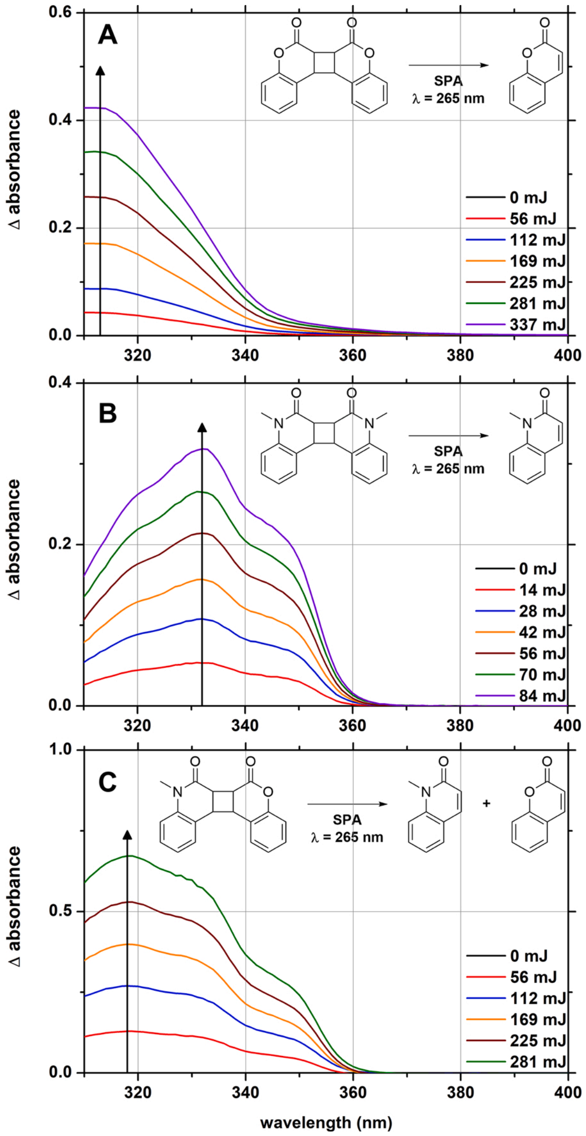

Fig. 3. SPA-cyclobutane cleavage of coumarin dimer (A), NMQ dimer (B) and NMQ/coumarin cross-dimer (C).

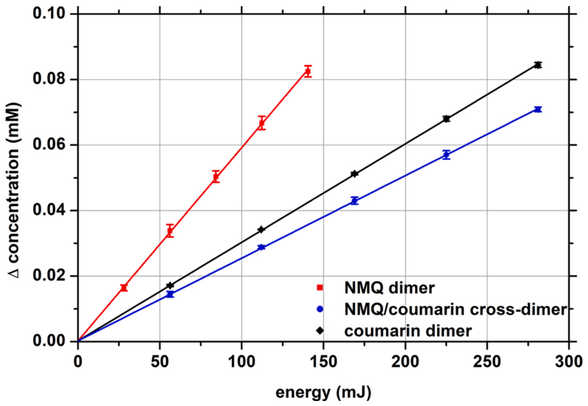

Fig. 4. Increase of NMQ and coumarin monomer concentration depending on the applied light energy.

$$A(\lambda) = [\varepsilon_{NMQ} \cdot c_{NMQ} + \varepsilon_{coumarin} \cdot c_{coumarin}] \cdot d \tag{1}$$

A(λ) describes the absorption at a given wavelength, ε is the absorption coefficient, *c* the to be determined concentration, and *d* the pathlength of the cuvette. As cyclobutane cleavage of the cross-dimer leads to the formation of one NMQ and one coumarin molecule, these two concentrations are identical (c_{mono}). Transforming Eq. (1) gives:

$$A = c_{mono} \cdot d \cdot (\varepsilon_{NMQ} + \varepsilon_{coumarin}) \tag{2}$$

$$c_{mono} = \frac{A}{d \cdot (\varepsilon_{NMQ} + \varepsilon_{coumarin})} \tag{3}$$

The initial optical density at 265 nm of the three unirradiated dimer solutions was higher than 2, justifying the approximation that all of the photons are absorbed. Taking the small values of overall conversions (< 1 %) during the SPA induced cleavage into account, we assume pseudo-zeroth-order kinetics for cyclobutane splitting. The quinolinone homo-dimer undergoes cyclobutane cleavage much more efficiently. We expected the cross-dimer cleavage efficiency in between those of the homo-dimers, but the SPA cleavage rate constant and the quantum yield for the hybrid cross-dimer are the lowest of the three species (see Table 1). This finding cannot be explained by the cross-dimer's absorption characteristics as the value of its absorption coefficient lies in between those of the homo-dimers. Previous work demonstrated that the coumarin and quinolinone homo-dimers SPA cleavage mechanisms show large differences. The coumarin dimer was found to cleave into two singlet ground state monomers, quinolinone dimer cleavage leads to the formation of one ground state and one excited state quinolinone [18]. Based on the presented results, it can be suggested that the dimer cleavage of the hybrid cross-dimer follows a pathway similar to that of coumarin. Substitution of only one lactone unit to a lactam does not lead to a higher cleavage efficiency.

TPA induced cyclobutane cleavage. Irradiating dimer solutions with intense 532 nm pulses leads to cleavage of the cyclobutane ring. For coumarin dimers, the TPA-induced ring cleavage is described in earlier literature [12]. The cleavage of NMQ dimer and NMQ/coumarin cross-dimer, traced by UV/Vis spectroscopy, is shown in Fig. 5.

Table 1
Absorption coefficients at 265 nm, zeroth-order kinetics rate constants, SPA cleavage quantum yields and two-photon cross section for the three investigated dimers.

	NMQ homo-dimer	coumarin homo-dimer	NMQ/coumarin cross-dimer
$\varepsilon_{265\,nm}^{ACN}$ [L·mol^{-1}·cm^{-1}]	14,541	2028	7497
v_0 [mmol·s^{-1}]	$8.315 \cdot 10^{-4}$	$4.243 \cdot 10^{-4}$	$3.526 \cdot 10^{-4}$
Φ_{SPA}	0.26	0.13	0.11
σ_{TPA} [GM]	0.74 ± 0.10	0.39 ± 0.03	0.35 ± 0.05

Both investigated dimers undergo cycloreversion upon irradiation with 532 nm laser pulses, which can be derived from the increasing absorption above 300 nm. HPLC analysis showed that only the monomeric forms result from the irradiation and no major side reactions occur. Due to the different mechanisms and the intrinsically lower absorption probability, the photocleavage efficiency is much lower compared to the above described single-photon reaction. The energy needed to achieve similar conversions differs by six orders of magnitude between these two photochemical processes (mJ-range for SPA, kJ-range for TPA). Compared to the results achieved via SPA induced cyclobutane cleavage, TPA cleavage of the homo-dimer is more efficient than that of the cross-dimer. As the photophysical process of two-photon reactions shows a quadratic dependence between monomer formation and irradiation intensity, the cycloreversion was investigated at different light intensities (Fig. 6) [28].

The reactions were carried out with laser pulses ranging from approximately 30 mJ/pulse to 100 mJ/pulse. For both, coumarin and quinolinone, an increased reaction rate can be observed with higher energy densities. The relation between the initial rate constant of conversion $v_0^{monomer}$ and the photon density F^2 with the initial dimer concentration c_0^{dimer}, the quantum yield for TPA cleavage Φ_{TPA} and the two-photon absorption cross-section σ_{TPA} in Goeppert-Mayer (GM) is given in Eq. 5.

$$v_0^{monomer} = 2 \cdot c_0^{dimer} \cdot \Phi_{TPA} \cdot \sigma_{TPA} \cdot F^2 \tag{5}$$

As can be derived from this equation, a double logarithmic plot of $\ln v_0^{monomer}$ versus $\ln F$ should show a linear dependence between these two parameters with an expected slope of 2. Experimental values of 1.73 in the case of NMQ and 1.54 for the NMQ/coumarin cross-dimer were obtained (Fig. 7). This dependence confirms the two-photon nature of the underlying process. As the occurrence of additional absorption processes via excited states cannot be excluded, the theoretical value of 2 for the slope is not obtained. The TPA cross-section σ_{TPA}, a parameter comparable to the absorption coefficient ε for SPA experiments, can be derived from Eq. 1. For the evaluation of the results, it is assumed that the quantum yield for dimer cleavage is the same for SPA and TPA experiments [12,29]. Considering the laser beam diameter, the effective reaction volume, and the effective reaction time, the TPA cross-sections of the investigated structures can be calculated to be 0.74 GM (NMQ dimer), 0.39 GM (coumarin dimer), and 0.35 GM (NMQ/coumarin cross-dimer). Comparing these values as well as the rate constants for dimer cleavage, presented in Fig. 7(B), it is obvious that the cross-dimer shows the lowest cleavage efficiency of the investigated structures, just like in single-photon cleavage.

This behavior can be explained by molecular symmetry considerations. Structures with a given donor-acceptor-donor π center and high symmetry reportedly show improved two-photon absorption characteristics compared to structures lacking these features [30,31]. The lactam function in the quinolinone homo-dimer acts as an electron donating group, the unsaturated cyclobutane in the chromophores center may be assigned as the electron-accepting part. In the case of the coumarin dimer, the lactone functions have a weaker electron-donating effect, explaining the lower two-photon-absorption cross-section as well as the lower rate constant for dimer cleavage. The even lower values for the cross-dimer are consistent with this explanation. An overall lower electron density compared to the NMQ dimer as well as the missing symmetry within this structure leads to a rather unfavorable two-photon-absorption process.

4. Conclusion

The presented experiments on *anti*-head-to-head coumarin and quinolinone (NMQ) homo-dimers, as well as the corresponding *anti*-head-to-head quinolinone-coumarin cross-dimer, studied the influence of the

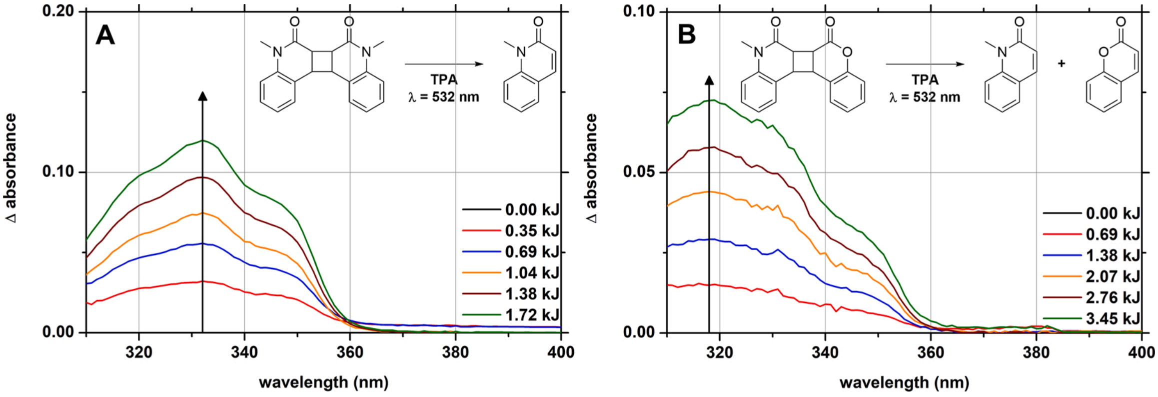

Fig. 5. TPA cyclobutane cleavage of NMQ dimer (A) and NMQ/coumarin cross-dimer (B).

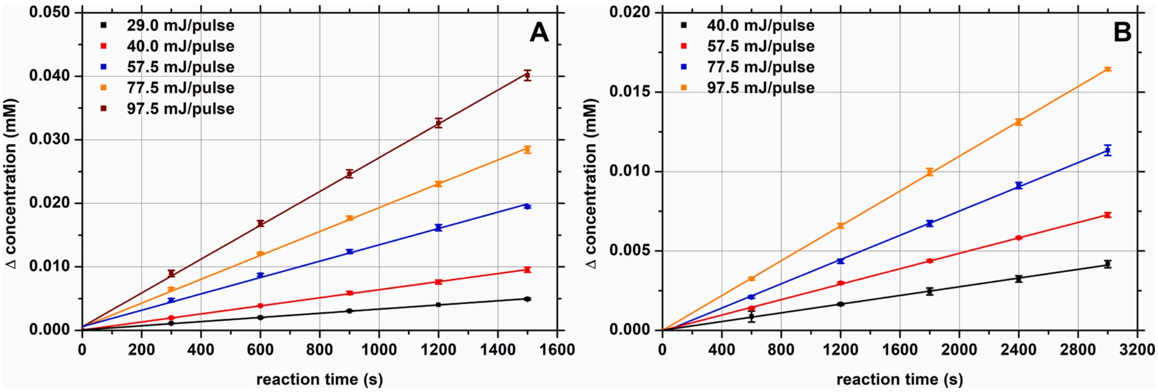

Fig. 6. TPA induced cyclobutane cleavage: Increase of the monomer concentration during TPA induced cyclobutane cleavage of NMQ dimer (A) and NMQ/coumarin cross-dimer (B) at different pulse energies.

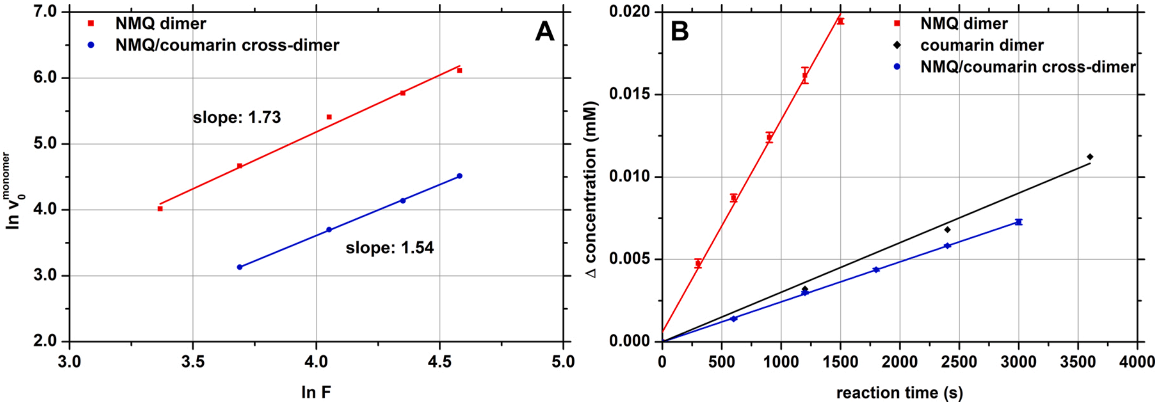

Fig. 7. (A) TPA induced photocleavage for the two considered dimers corresponds with the slope of 1.73 and 1.54 in the double logarithmic plot. (B) Comparison of the rate constants for dimer cleavage of the investigated three dimers at 57.5 mJ/pulse. (Error bars are in some cases smaller than the symbols.).

cyclobutane substitution pattern on the single-photon and two-photon absorption induced dimer cleavage efficiency. Dimers of the lactam-analog of the lactone coumarin, the quinolinone dimer, shows significantly improved cycloreversion rates, both in single-photon as well as in two-photon experiments. The quantum yield for SPA dimer cleavage (0.26) and the two-photon-absorption cross-section (0.74 GM) are both about 2-fold higher than the corresponding coumarins values. The more efficient cyclobutane cleavage makes the quinolinone framework an advantageous structure for various applications like photo cross-linkable polymers. It was expected that the values for a mixed hybrid dimer, carrying one lactone and one lactam moiety, to lie somewhere in between those of the corresponding homo-dimers. We found that the cross-dimer shows lower cleavage efficiency in both single- and two-photon experiments compared to both homo-dimers. This behavior is explained through a lack of molecular symmetry in the NMQ/coumarin cross-dimer. It may be postulated that homo-dimers show higher single- and two-photon absorption induced cycloreversion rates compared to cross-dimers.

Author statement

All authors contributed equally to the manuscript.

All authors are aware of the revised manuscript.

Declaration of Competing Interest

The authors declare that they have no known competing financial interests or personal relationships that could have appeared to influence the work reported in this paper.

References

[1] G. Ciamician, P. Silber, Chemische lichtwirkungen, Berichte der Dtsch. Chem. Gesellschaft. 35 (1902) 4128–4131, https://doi.org/10.1002/cber.19110440252.

[2] C.H. Krauch, S. Farid, G.O. Schenck, Photo-C4-Cyclodimerisation von cumarin, Chem. Ber. 99 (1966) 625–633, https://doi.org/10.1002/cber.19660990237.

[3] G.S. Hammond, C.A. Stout, A.A. Lamola, Mechanisms of photochemical reactions in solution. XXV. The photodimerization of coumarin, J. Am. Chem. Soc. 86 (1964) 3103–3106, https://doi.org/10.1021/ja01069a026.

[4] N. Yonezawa, T. Yoshida, M. Hasegawa, Symmetric and asymmetric photocleavage of the cyclobutane rings in head-to-head coumarin dimers and their lactone-opened derivatives, J. Chem. Soc. Perkin Trans. I 1 (1983) 1083–1086, https://doi.org/10.1039/P19830001083.

[5] Y. Chen, J.-L. Geh, Copolymers derived from 7-acryloyloxy-4-methylcoumarin and acrylates: 2. Reversible photocrosslinking and photocleavage, Polymer (Guildf). 37 (1996) 4481–4486, https://doi.org/10.1016/0032-3861(96)00300-X.

[6] M. Schadt, H. Seiberle, A. Schuster, Optical patterning of multi-domain liquid-crystal displays with wide viewing angles, Nature 381 (1996) 212–215, https://doi.org/10.1038/381212a0.

[7] N.K. Mal, M. Fujiwara, Y. Tanaka, Photocontrolled reversible release of guest molecules from coumarin-modified mesoporous silica, Nature 421 (2003) 350–353, https://doi.org/10.1038/nature01362.

[8] S. Härtner, H.-C. Kim, N. Hampp, Phototriggered release of photolabile drugs via two-photon absorption-induced cleavage of polymer-bound dicoumarin, J. Polym. Sci. Part A: Polym. Chem. 45 (2007) 2443–2452, https://doi.org/10.1002/pola.22007.

[9] M. Jiang, N. Paul, N. Bieniek, T. Buckup, N. Hampp, M. Motzkus, Photocleavage of coumarin dimers studied by femtosecond UV transient absorption spectroscopy, Phys. Chem. Chem. Phys. 19 (2017) 4597–4606, https://doi.org/10.1039/C6CP08076F.

[10] T. Wolff, H. Görner, Photocleavage of dimers of coumarin and 6-alkylcoumarins, J. Photochem. Photobiol. A: Chem. 209 (2010) 219–223, https://doi.org/10.1016/j.jphotochem.2009.11.018.

[11] T. Buckup, A. Southan, H.C. Kim, N. Hampp, M. Motzkus, Optimisation of two-photon induced cleavage of molecular linker systems for drug delivery, J. Photochem. Photobiol. A: Chem. 210 (2010) 188–192, https://doi.org/10.1016/j.jphotochem.2009.12.016.

[12] H.C. Kim, S. Kreiling, A. Greiner, N. Hampp, Two-photon-induced cycloreversion reaction of coumarin photodimers, Chem. Phys. Lett. 372 (2003) 899–903, https://doi.org/10.1016/S0009-2614(03)00535-9.

[13] M. Patel, R.J. McHugh Jr., B.C. Cordova, R.M. Klabe, L.T. Bacheler, S. Erickson-Viitanen, J.D. Rodgers, Synthesis and evaluation of quinolinones as HIV-1 reverse transcriptase inhibitors, Bioorg. Med. Chem. 11 (2001) 1943–1945, https://doi.org/10.1002/chin.200045170.

[14] P. Hradil, J. Hlavac, M. Soural, M. Hajduch, M. Kolar, R. Vecerova, 3-hydroxy-2-phenyl-4(1H)-quinolinones as promising biologically active compounds, Mini-Reviews Med. Chem. 9 (2009) 696–702, https://doi.org/10.2174/138955709788452720.

[15] P. Barraja, P. Diana, A. Montalbano, G. Dattolo, G. Cirrincione, G. Viola, D. Vedaldi, F. Dall'Acqua, Pyrrolo[2,3-h]quinolinones: A new ring system with potent photoantiproliferative activity, Bioorg. Med. Chem. Lett. 14 (2006) 8712–8728, https://doi.org/10.1016/j.bmc.2006.07.061.

[16] F.D. Lewis, G.D. Reddy, J.E. Elbert, B.E. Tillberg, J.A. Meltzer, M. Kojima, Spectroscopy and photochemistry of 2-Quinolones and their lewis acid complexes, J. Org. Chem. 56 (1991) 5311–5318, https://doi.org/10.1021/jo00018a020.

[17] H. Görner, T. Wolff, Lewis-acid-catalyzed photodimerization of coumarins and N-methyl-2-quinolone, Photochem. Photobiol. 84 (2008) 1224–1230, https://doi.org/10.1111/j.1751-1097.2008.00339.x.

[18] N. Paul, M. Jiang, N. Bieniek, J.L.P. Lustres, Y. Li, N. Wollscheid, T. Buckup, A. Dreuw, N. Hampp, M. Motzkus, Substituting coumarins for quinolinones: altering the cycloreversion potential energy landscape, J. Phys. Chem. A 122 (2018) 7587–7597, https://doi.org/10.1021/acs.jpca.8b07186.

[19] A. Angeli, E. Trallori, F. Carta, L. Di Cesare Mannelli, C. Ghelardini, C.T. Supuran, Heterocoumarins are selective carbonic anhydrase IX and XII inhibitors with cytotoxic effects against Cancer cells lines, ACS Med. Chem. Lett. 9 (2018) 947–951, https://doi.org/10.1021/acsmedchemlett.8b00362.

[20] H.J. Kuhn, S.E. Braslavsky, R. Schmidt, Chemical actinometry (IUPAC technical report), Pure Appl. Chem. 76 (2004) 2105–2146, https://doi.org/10.1351/pac200476122105.

[21] V. Ladányi, P. Dvořák, J. Al Anshori, Ľ. Vetráková, J. Wirz, D. Heger, Azobenzene photoisomerization quantum yields in methanol redetermined, Photochem. Photobiol. Sci. 16 (2017) 1757–1761, https://doi.org/10.1039/c7pp00315c.

[22] T. Hartman, R. Cibulka, Photocatalytic systems with flavinium salts: from photolyase models to synthetic tool for cyclobutane ring opening, Org. Lett. 18 (2016) 3710–3713, https://doi.org/10.1021/acs.orglett.6b01743.

[23] S. Inacker, N. Bieniek, N.A. Hampp, K. Harms, CCDC 2055301: experimental crystal structure determination, CSD Commun. (2021), https://doi.org/10.5517/ccdc.csd.cc26zq1z.

[24] C.P. Haas, S. Biesenroth, S. Buckenmaier, T. Van De Goor, U. Tallarek, Automated generation of photochemical reaction data by transient flow experiments coupled with online HPLC analysis, React. Chem. Eng. 5 (2020) 912–920, https://doi.org/10.1039/d0re00066c.

[25] S. Inacker, N. Bieniek, N.A. Hampp, S.I. Ivlev, CCDC 2056124: experimental crystal structure determination, CSD Commun. (2021), https://doi.org/10.5517/ccdc.csd.cc270klf.

[26] V. Ladányi, P. Dvořák, J. Al Anshori, Ľ. Vetráková, J. Wirz, D. Heger, Azobenzene photoisomerization quantum yields in methanol redetermined, Photochem. Photobiol. Sci. 16 (2017) 1757–1761, https://doi.org/10.1039/C7PP00315C.

[27] M. Hasegawa, Y. Suzuki, N. Kita, Photocleavage of coumarin dimers, Chem. Lett. 1 (1972) 317–320, https://doi.org/10.1246/cl.1972.317.

[28] M. Göppert-Mayer, Über elementarakte mit Zwei Quantensprüngen, Ann. Phys. 401 (1931) 273–294, https://doi.org/10.1002/andp.19314010303.

[29] L. Parma, N. Omenetto, Two-photon absorption of 7-hydroxycoumarine, Chem. Phys. Lett. 54 (1978) 541–543, https://doi.org/10.1016/0009-2614(78)85280-4.

[30] C.K. Wang, P. Macak, Y. Luo, H. Ågren, Effects of π centers and symmetry on two-photon absorption cross sections of organic chromophores, J. Chem. Phys. 114 (2001) 9813–9820, https://doi.org/10.1063/1.1371258.

[31] N. Hobeika, H. Chaumeil, R. Mhanna, M. Jin, X. Wu, A. Spangenberg, D. Versace, F. Morlet-Savary, J. Malval, Two-photon initiating efficiency of a ditopic alkoxynitrostilbene reacting through a self-regenerative mechanism, Chem. Phys. Chem. 21 (2020) 2301–2310, https://doi.org/10.1002/cphc.202000437.